Microglial Acid Sensing Regulates Carbon Dioxide Evoked Fear

Supplemental Information

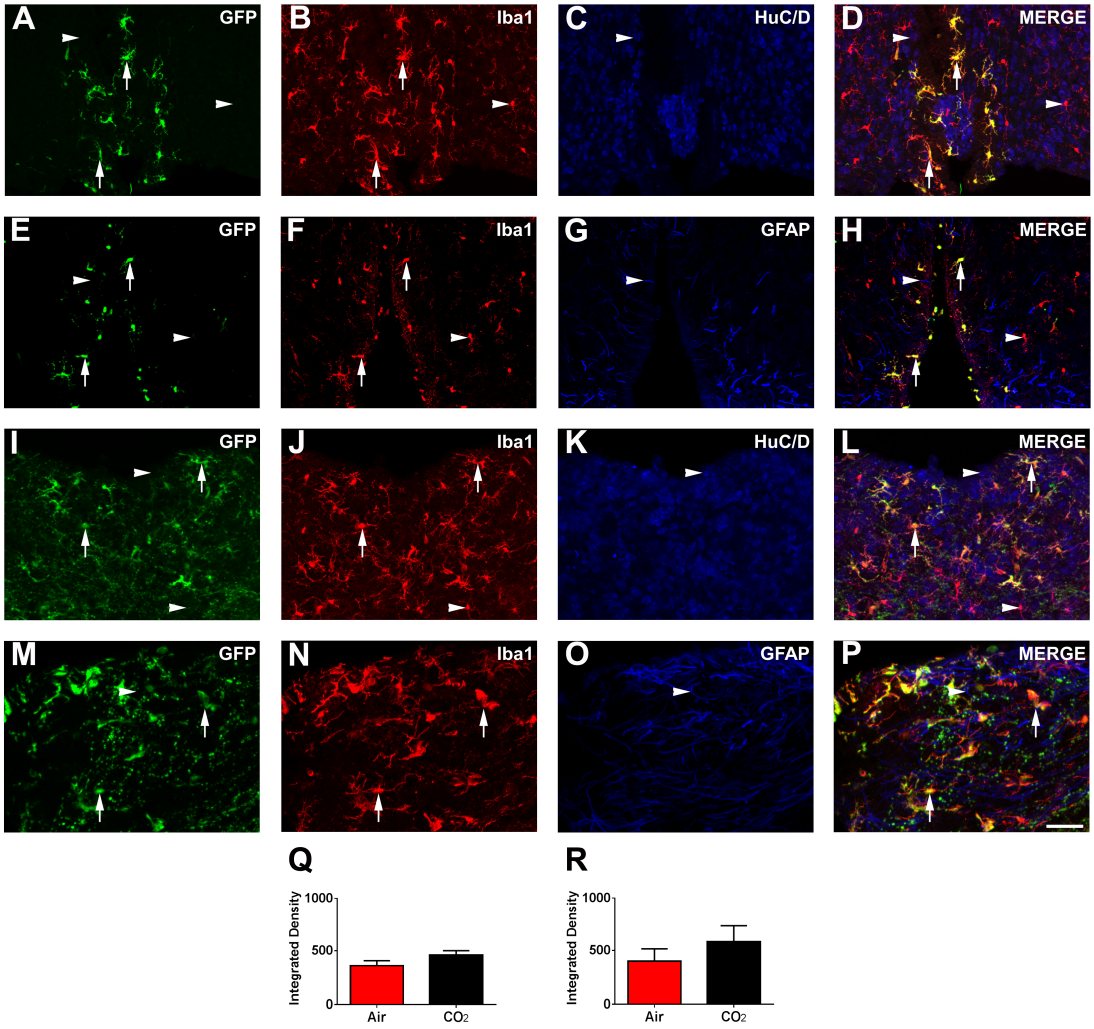

Figure S1. Microglia within the sensory circumventricular organs, organum vasculosum of lamina terminalis (OVLT; panels **A-H**) and area postrema (AP; panels **I-P**) express acid-sensing T cell death associated gene-8 (TDAG8) receptor. GFP-positive cells (panels **A, E, I, M**) co-localized with IBA-1-positive microglia (panels **B, F, J** and **N**). (Co-localized cells are shown in panels **D, H, L, P** by arrows). GFP-labeled cells do not localize with HuC/D-positive neurons (panels **C, K**) or GFAP-positive astrocytes (panels **G,O**). CO_2-inhalation had no significant effect on TDAG8 promoter-controlled GFP expression in the OVLT (**Q**) or AP (**R**). No significant change in GFP expression (integrated density) as compared to the air inhalation group was observed. (unpaired *t* test OVLT: $t_{(9)} = 0.1327$; AP: $t_{(16)} = 0.3719$, $p > .05$ vs air). Double labeled GFP-IBA-1 cells are indicated by arrows. Single labeled cells are indicated by arrowheads. (Scale bar = 20 µm).

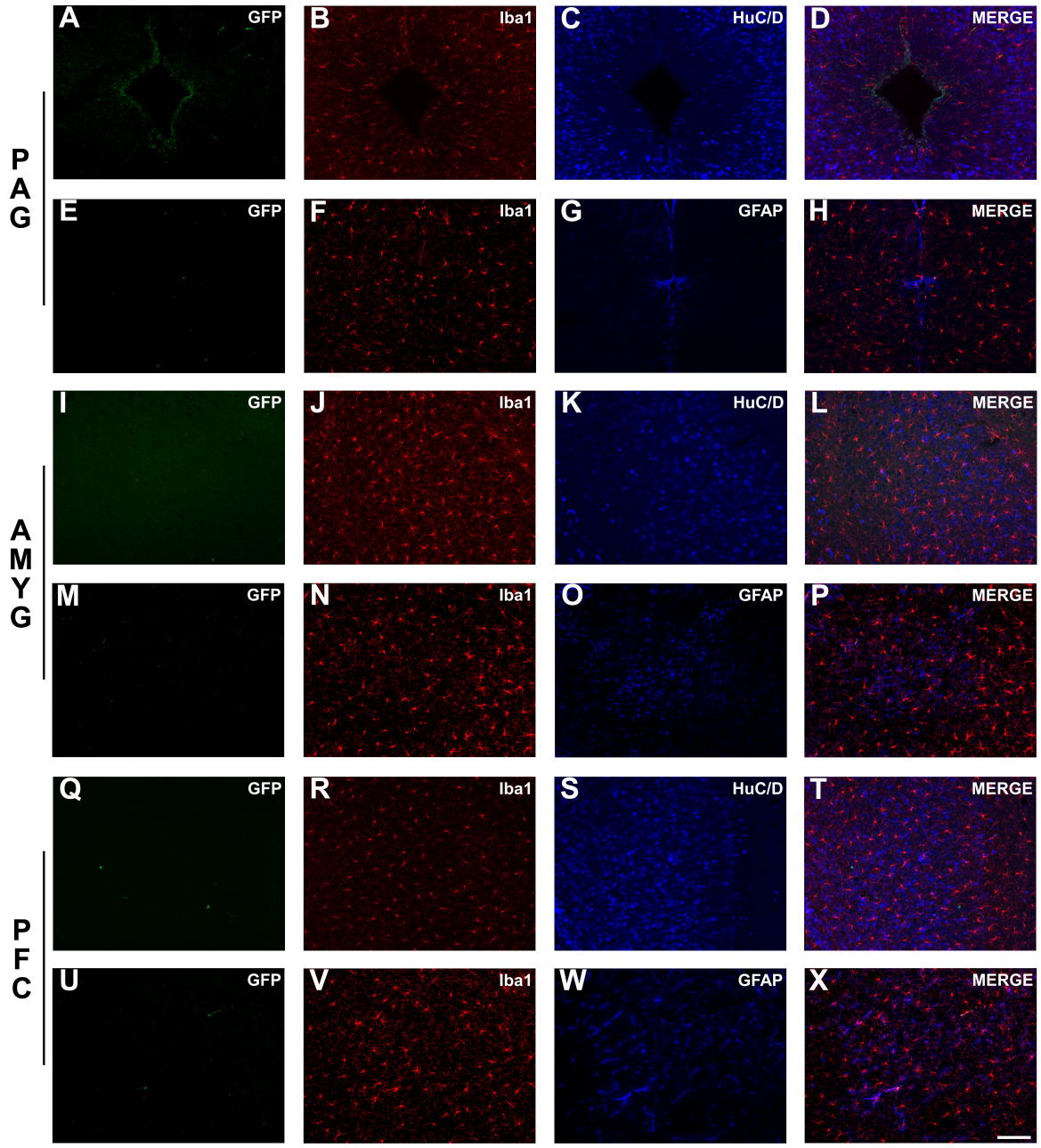

Figure S2. Triple immunostaining revealed negligible expression of TDAG8 promoter-driven GFP-positive cells in brain regions relevant to fear regulation such as the periaqueductal grey (PAG) (panels **A-H**), amygdala (AMYG) (panels **I-P**) and prefrontal cortex (PFC) (panels **Q-X**). Although no GFP expression was observed, numerous IBA-1-positive microglia, HuC/D-positive neurons and GFAP-positive astrocytes were observed in each region (scale bar = 10 μm).

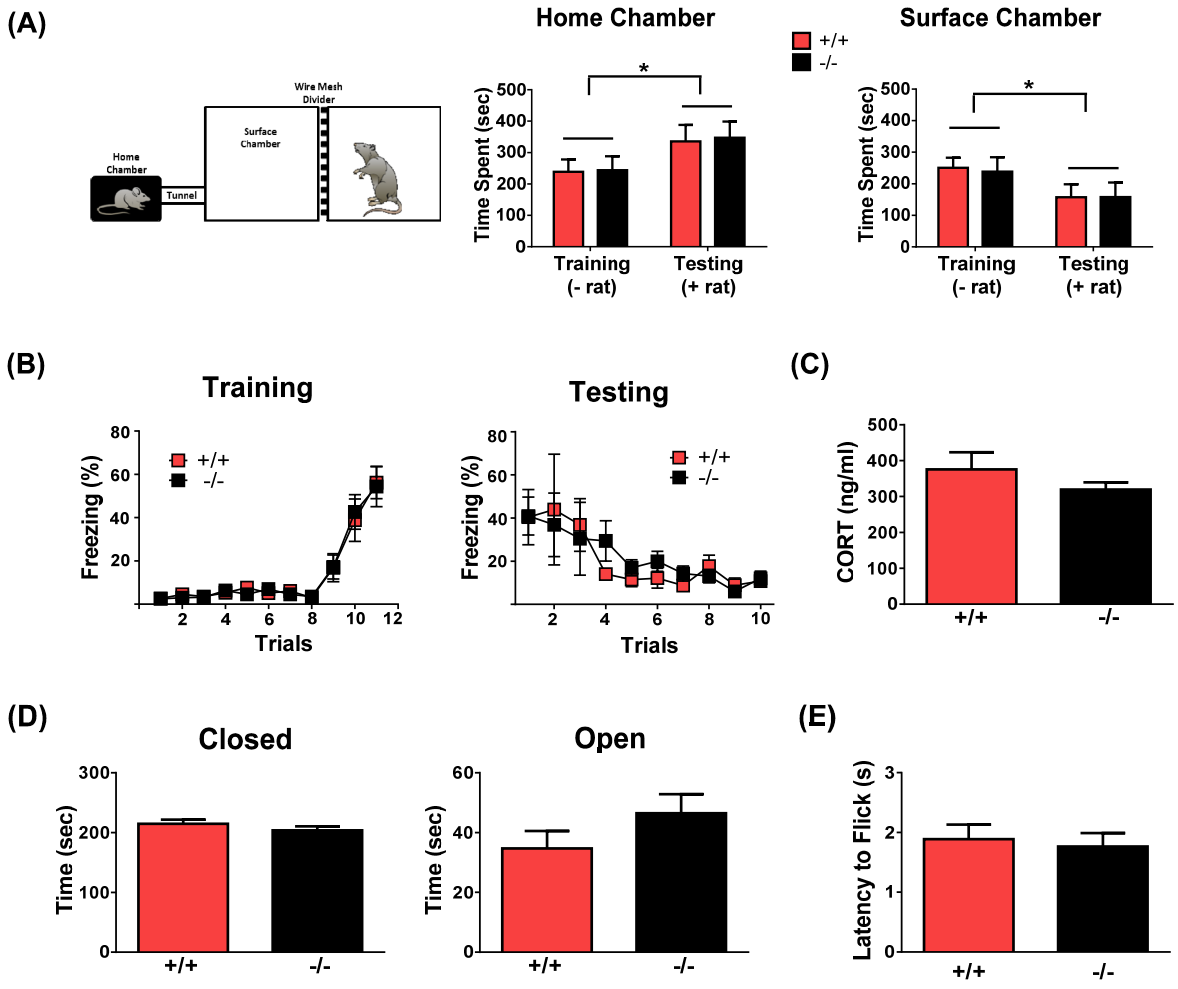

Figure S3. TDAG8$^{-/-}$ mice show similar responses to exteroceptive fearful stimuli in comparison with TDAG8$^{+/+}$ mice. (**A**) Exposure to the rat exposure test (RET; see illustration), simulating threat evoked by a predator, produced similar defensive behaviors in TDAG8$^{+/+}$ and $^{-/-}$ mice. Time spent in the home, surface chambers and tunnel section of the apparatus was measured. Two way ANOVA revealed no significant effect of genotype (mean ± SEM, two-way ANOVA, $F_{(2,36)}$ = 0.00001; p > .05, n = 8 mice). However, a significant effect of time spent between chambers was observed (mean ± SEM, two-way ANOVA, $F_{(2,36)}$ = 19.75; p < .05, n = 8 mice), as mice elicit preference for the home chamber as compared to the surface chamber. (**B**) Cued fear conditioning in TDAG8$^{+/+}$ and $^{-/-}$ mice. Amount of freezing was determined during training and testing for conditioned fear and extinction. No significant difference in freezing was observed between $^{+/+}$ and $^{-/-}$ mice during training and testing. Training data revealed a significant effect of trial (two-way repeated measures ANOVA $F_{(10,176)}$ = 27.57; p < .05, n = 10), but no genotype ($F_{(1,176)}$ = 0.32; p > .05, n = 10) or genotype x trial interaction ($F_{(10,176)}$ = 0.07; p > .05, n = 10). For testing data, a significant effect of trial (two-way repeated measures ANOVA, $F_{(9,110)}$ = 3.237; p < .05, n = 10), but no genotype ($F_{(1,110)}$ = 0.116; p > .05, n = 10) or genotype x trial interaction ($F_{(1,110)}$ = 0.264; p > .05, n = 10) was observed. TDAG8$^{-/-}$ mice elicit similar reactivity

in hypothalamic pituitary adrenal (HPA) response to restraint stress (**C**), on exposure to the elevated plus maze (EPM) (**D**), and tail flick test (TFT) (**E**). Neuroendocrine response following exposure to one hour of restraint stress revealed no significant difference in plasma corticosterone (CORT) concentrations between TDAG8$^{+/+}$ and $^{-/-}$ mice (mean ± SEM, $p > .05$; Student t test, $n = 10$/genotype). No significant differences were observed in time spent in both the closed and open arms of the EPM (mean ± SEM, $p > .05$, Student t test, $n = {}^{+/+}13$, $^{-/-}12$). TDAG8$^{-/-}$ mice elicited no significant difference in latency time to flick following a thermal stress (mean ± SEM, $p > .05$; Student t test, $n = 9$/genotype).

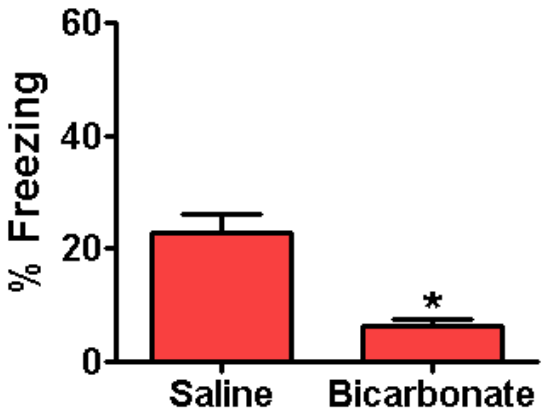

Figure S4. Bicarbonate (HCO_3^-) administration attenuates CO_2-evoked freezing. HCO_3^- (2 mM/kg, i.p.) administered prior to CO_2 inhalation reduced CO_2-evoked freezing in BALBc mice. ($n = 6$). Data are mean ± SEM, $^*p < .05$ vs saline.

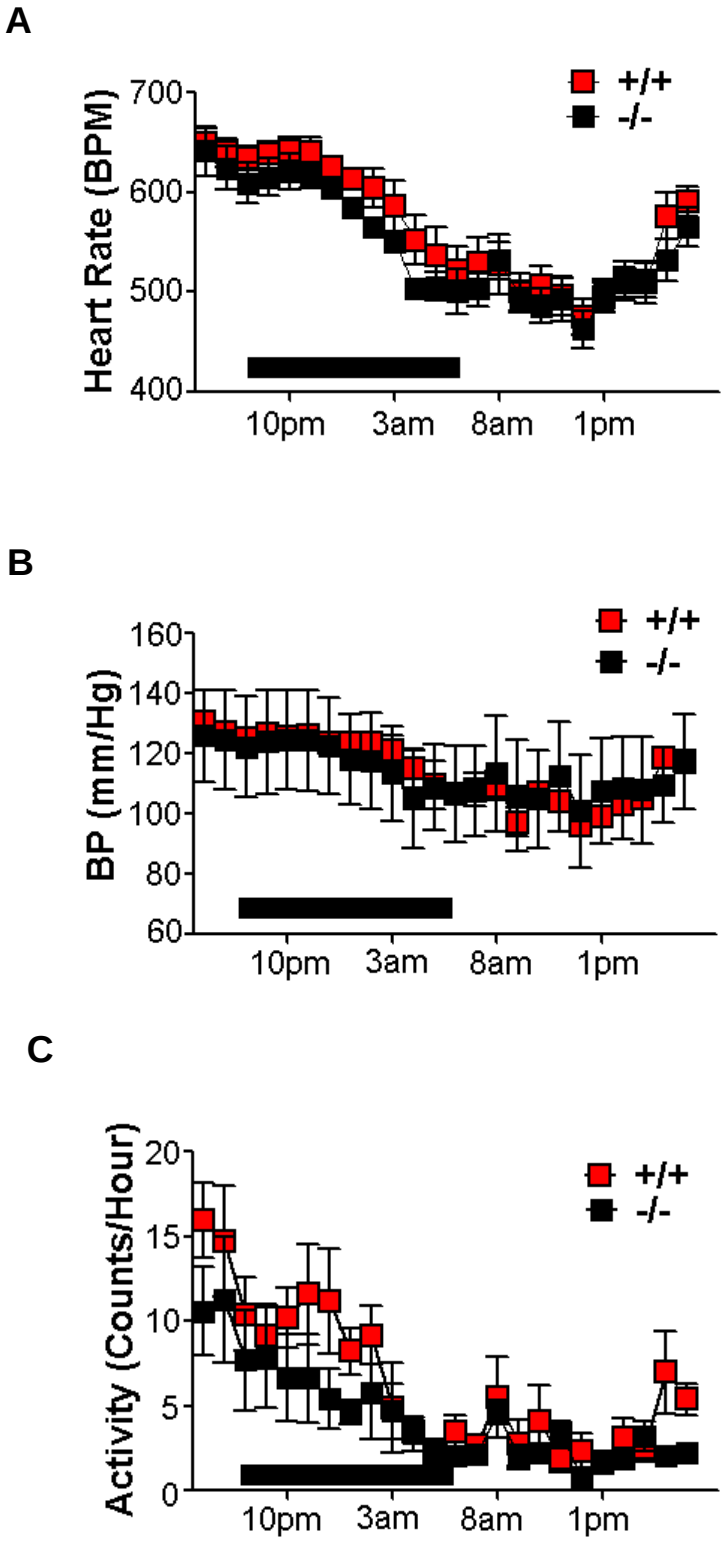

Figure S5. Cardiovascular measures and locomotor activity of TDAG8$^{+/+}$ and $^{-/-}$ mice at baseline (**A-C**). Following recovery, mice with telemetric implants were monitored for a period of 4 days prior to experimentation. Baseline recordings of heart rate (**A**) and blood pressure (**B**) revealed

a significant effect of time for heart rate [two-way RM ANOVA, $F_{(23,184)}$ = 40.80; p < .0001, n = 5/group] and blood pressure [two-way RM ANOVA, $F_{(23,161)}$ = 17.98; p < .0001]. However, no significant effect of genotype for heart rate [$F_{(1,184)}$ = 1.08, p = .329] or blood pressure [$F_{(1,161)}$ = 0.0012, p = .973] was observed. (**C**) Locomotor activity of $^{+/+}$ and $^{-/-}$ mice was not significantly different (genotype: two-way RM ANOVA, $F_{(1,161)}$ = 2.65; p = .147, n = 5). However, a significant effect of time ($F_{(23,161)}$ = 9.31; p < .0001, n = 5) was observed. All data are mean ± SEM.

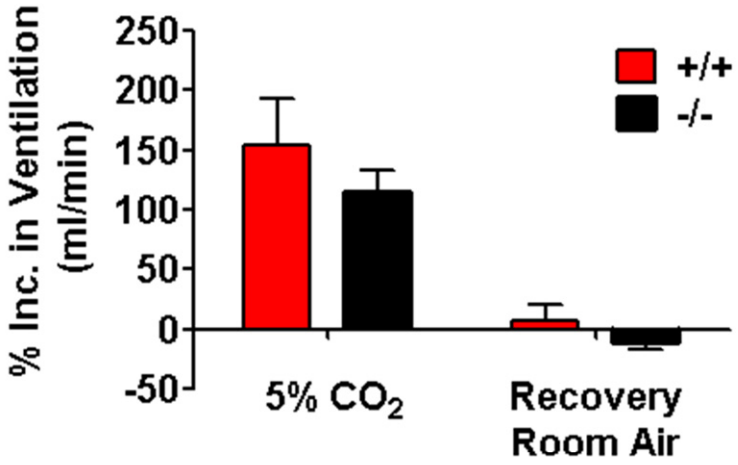

Figure S6. Ventilatory responses to carbon dioxide (CO_2) inhalation and post inhalation recovery in TDAG8$^{+/+}$ and $^{-/-}$ mice using whole body plethysmography. A significant (100-150%) increase in ventilatory rate (V_E) was observed in both $^{+/+}$ and $^{-/-}$ mice that was not significantly different from each other. Upon return to room air, V_E was restored to initial values in both genotypes with no significant differences. Two-way ANOVA revealed a significant effect of treatment [$F_{(1,28)}$ = 43.94; p < .0001, n = 7 ($^{+/+}$), n = 9 ($^{-/-}$)], but not effect of genotype [$F_{(1,28)}$ = 1.83; p = .187, n = 7 ($^{+/+}$), n = 9 ($^{-/-}$)]. All data are mean ± SEM.

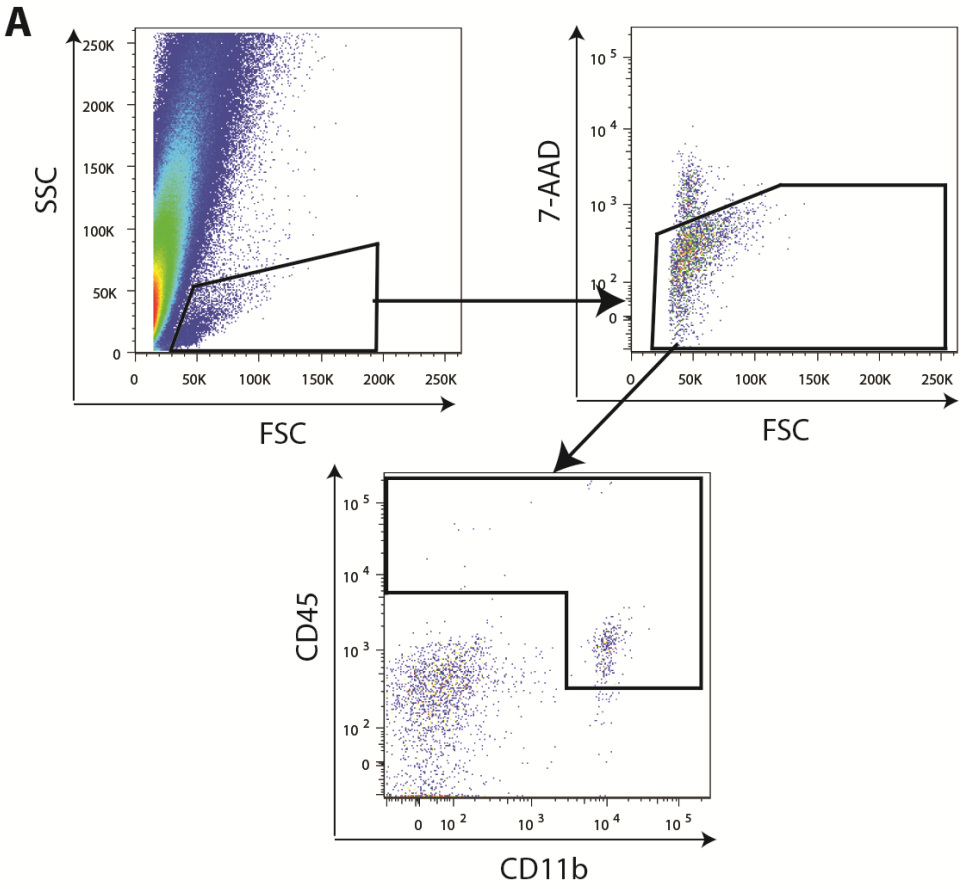
A
SSC
FSC
7-AAD
FSC
CD45
CD11b
B
Air exposed
CO_2 exposed
CD45
Macrophages (2.8%)
Microglia (95.5%)
Macrophages (3.2%)
Microglia (95.1%)
CD11b
C
Microglia ($CD45^{low}$)
Macrophages ($CD45^{high}$)
% SFO Myeloid Cells (CD11b+)
Air
CO_2

Figure S7. Flow cytometry analysis of myeloid cells within the SFO. (**A**) Gating strategy to identify microglia and macrophages within the SFO. SFO-enriched tissue was dissected from the brains of air- and CO_2-exposed animals 24 h post inhalation. Cells were stained as described in the Methods and Materials section. (**A**) FSC versus SSC gating was used to isolate cells from myelin debris, live cells were identified on the basis of 7-AAD exclusion, and microglial and macrophage cells were identified on the basis of CD45 and/or CD11b positivity. (**B**) Macrophages ($CD45^{high}$, $CD11b^{+}$), and microglia ($CD45^{low}$, $CD11b^{+}$) were identified from air-exposed (left panel) or 5% CO_2-exposed (right panel) animals. A single representative plot from n = 7-12 animals/group is shown. (**C**) Percentage of: microglia ($CD45^{low}$) and macrophages ($CD45^{high}$) within the subfornical organ in air and CO_2 exposed groups. Myeloid cells within the SFO were predominantly $CD45^{low}$ microglia (>95%) as compared to $CD45^{high}$ macrophages (<5%) in the air inhalation group. Importantly, this ratio did not change following inhalation of 5% CO_2. Two-way ANOVA revealed no significant effect of treatment [$F_{(1,35)}$ = 0.000001; p = .9975, n = 12 (air), n = 7 (CO_2)], but a significant effect of cell type [$F_{(1,35)}$ = 1427; p < .0001] was observed. All data are mean ± SEM.

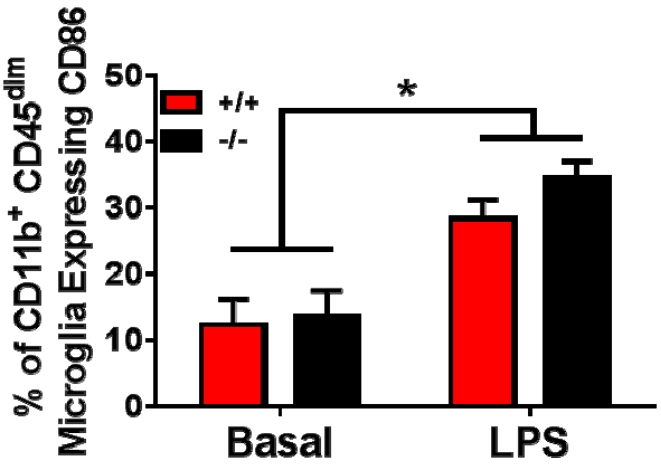

Figure S8. LPS-evoked microglial activation is intact in TDAG8$^{-/-}$ mice. TDAG8$^{+/+}$ and $^{-/-}$ mice were injected i.p. with LPS (0.5 mg/kg). Brain tissue was collected 4 h post treatment. Microglial activation in brain was assessed by flow cytometry. LPS resulted in a significant increase in the frequency of CD11b^{+} CD45^{low} microglia expressing CD86 in both genotypes. Two way ANOVA revealed a significant effect of treatment [$F_{(1,25)}$ = 32.41; p < .05] but no significant effects of genotype or a treatment x genotype interaction. *p < .05.

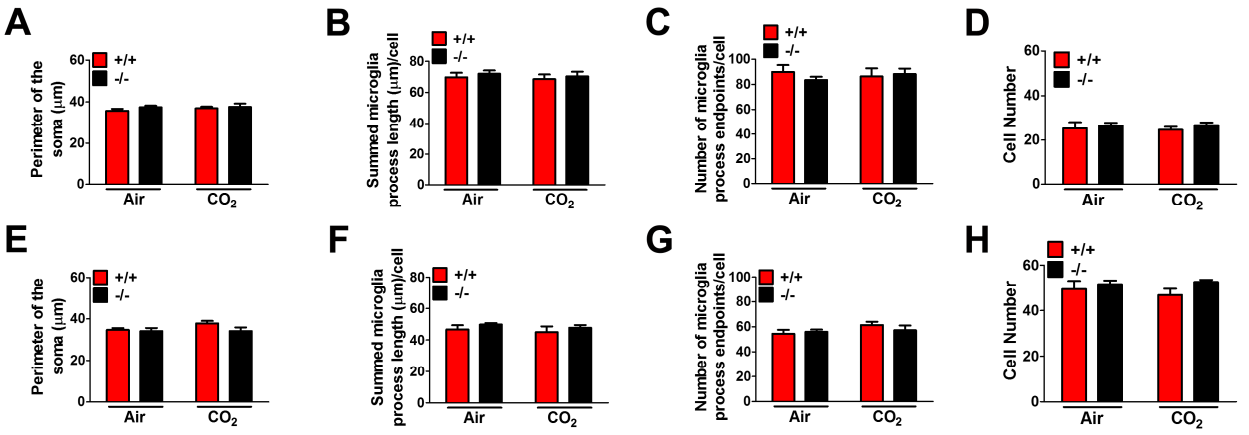

Figure S9. No significant difference in any of the microglial parameters were observed within other CVOS: the OVLT (panels **A-D**) and area postrema (panels **E-H**). All data are mean ± SEM. From 3 slices/animal/group. *n* = 6/group.

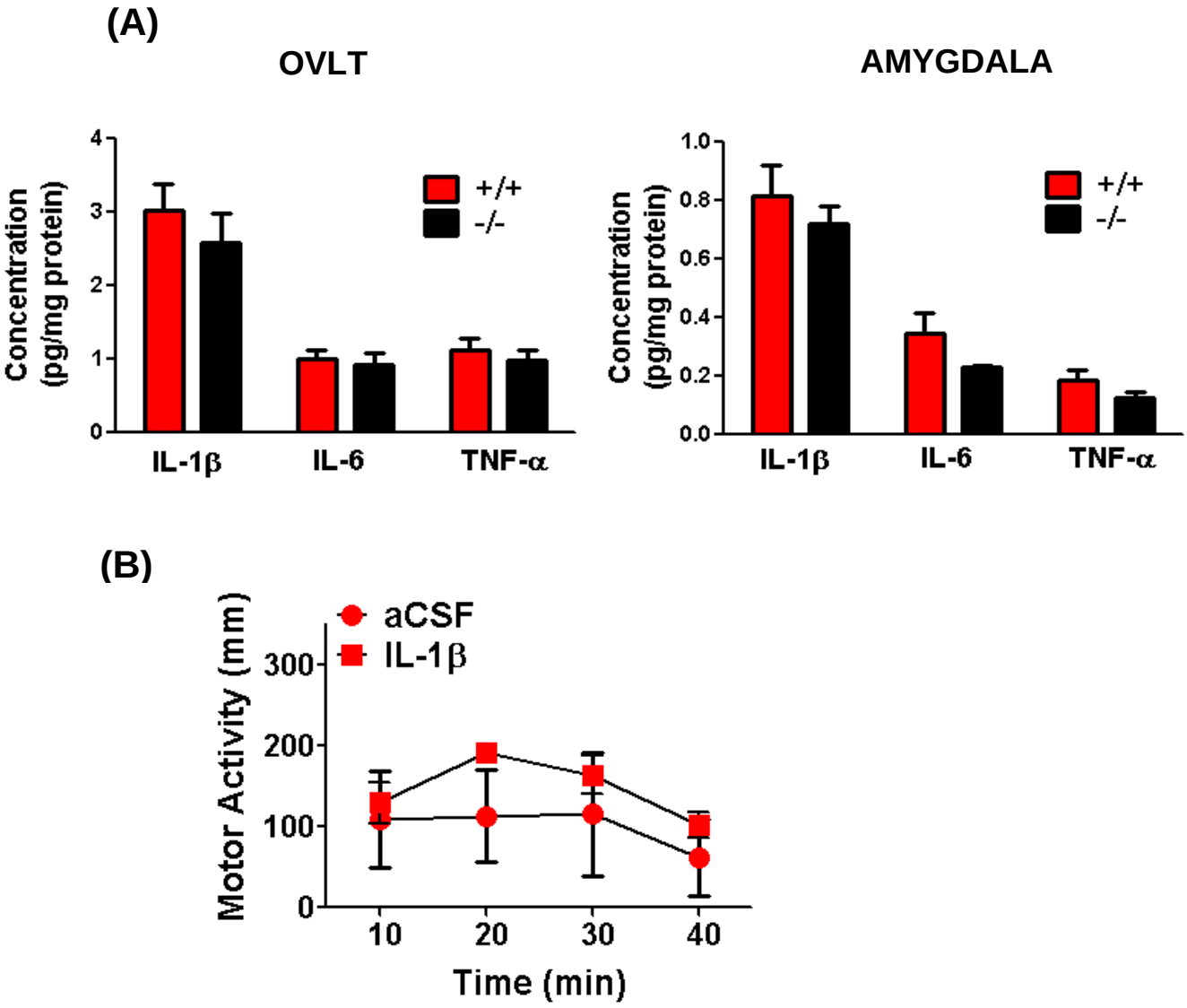

Figure S10. Concentration of pro-inflammatory cytokines, IL-1β, IL-6 and TNFα within the OVLT and amygdala (**A**). No significant differences in cytokine levels were observed between genotypes (*n* = 4). (**B**) Central i.c.v. infusion of interleukin 1β (IL-1β) does not cause significant changes in motor activity over the time interval for behavioral testing. No significant effect of treatment was observed. All behavioral experiments post IL-1β in fusion were conducted (<30 min) ruling out direct effects of IL-1β on immobility/freezing behavior post CO_2 inhalation. All data are mean ± SEM.

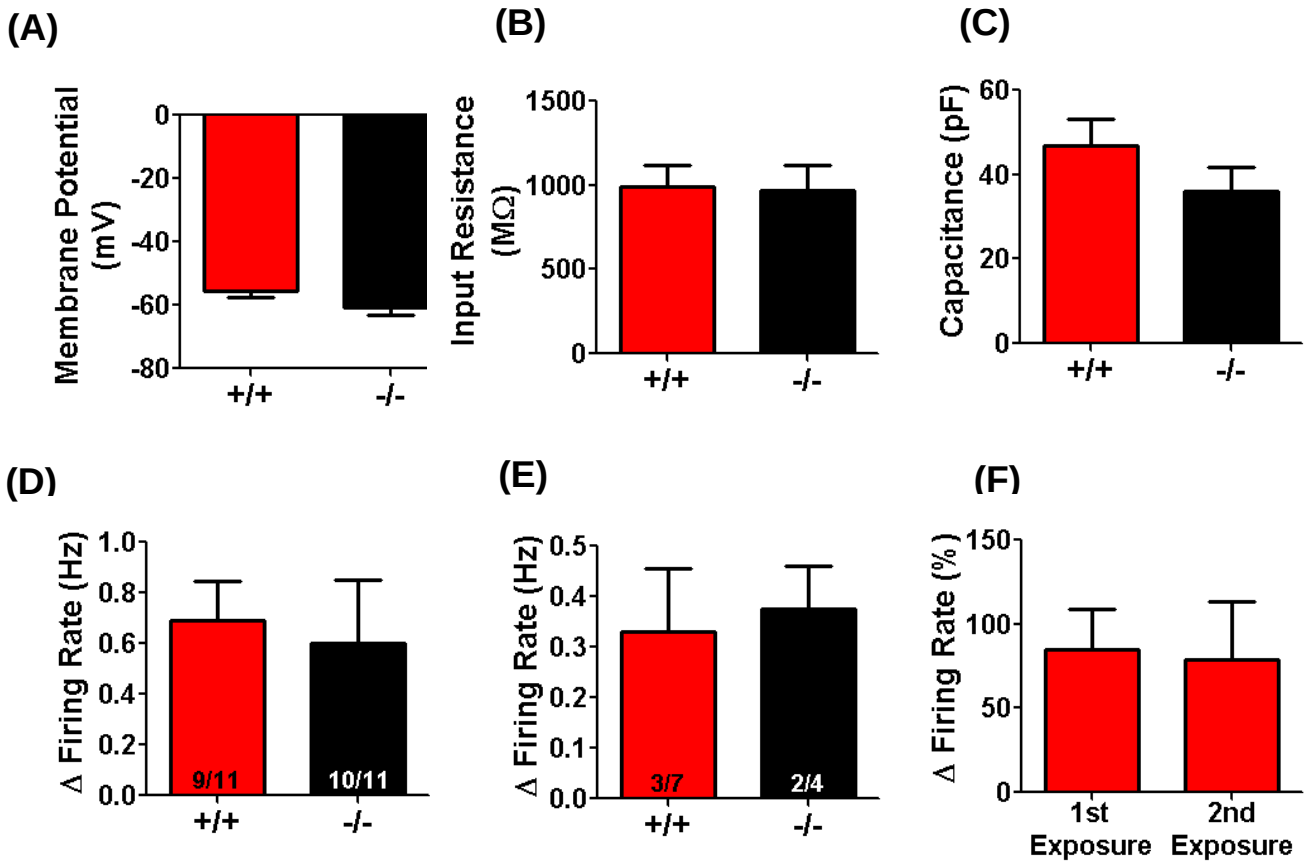

Figure S11. Intrinsic membrane properties of SFO neurons do not differ between TDAG8$^{+/+}$ and TDAG8$^{-/-}$animals. (**A**) Membrane potential, (**B**) input resistance, and (**C**) membrane capacitance are unaffected by TDAG8 deficiency (n = 8-9). (**D**) Firing rate increases of locus coeruleus (LC) neurons in response to elevated CO_2 does not differ between +/+ and -/- mice. Bars show ratio of CO_2-responsive neurons/total neurons (n = 9/11$^{+/+}$; n = 10/11$^{-/-}$). (**E**) Increase in firing rate in area postrema (AP) neurons also revealed no significant differences. Bars show ratio of CO_2-responsive neurons/total neurons (n = 3/7$^{+/+}$; n = 2/4$^{-/-}$). (**F**) Sequential application of 7.5% CO_2 can evoke increases in SFO neuron firing frequency. The change in firing frequency induced by exposing the neuron to 7.5% CO_2 does not differ between the first and second exposure (p > .05), enhancing confidence that IL-IRA evoked reduction of firing is due to altered CO_2-chemosensitivity and not an effect of reduced firing rate due to re-exposure. All data are mean ± SEM.

Supplemental Methods

CO_2 Inhalation Experiment Details

On the testing day (Day 1), air, 5% or 10% CO_2 (in 21% O_2, balance with N_2, Wright Brothers Inc., Cincinnati) was infused through a valve in the ceiling of the chamber (8“ x 8” x 6.5”) similar to a previous study (1) to avoid direct blowing of air/CO_2, which is aversive to rodents. This created a steady-state CO_2 concentration that was controlled by a flow meter to ensure a steady infusion rate of 10 L/min for all animals.

Surgery

Guide cannulae (26-gauge; Plastics One) were implanted into the lateral ventricle of anesthetized mice (coordinates: 0.46 mm posterior to bregma, 0.9 mm lateral from midline, and 1.3 mm dorsoventral from dura). Coordinates were selected to ensure drug administration near the vicinity of the subfornical organ (SFO) without damaging the structure. Initiation of treatment and behavioral testing occurred following one week recovery. Cannula placement was verified postmortem using cresyl violet staining.

Whole Body Plethysmography

The setup consisted of a 450 ml glass chamber with ports in the top for gas inflow and outflow. In addition we sealed a temperature probe (Physitemp HT-1 general purpose) into the top of the chamber to measure chamber temperature. Air was pumped through the inflow line by a Marina 100 Aquarium Air Pump. An air stone in a 125 ml Erlenmeyer flask containing 100 ml distilled water saturated the inflow air. The inflow air then was fed to an Aalborg rotameter (GMR3-010022) for the adjustment of the rate of air flow, which was measured by an in-line TSI 4100 Series mass flow meter. This meter also measured the ambient pressure. Finally, air passed through a Millipore in-line filter (6 cm diameter) before entering the chamber. The outflow air

was directed to a differential pressure transducer (TSD 160A, Biopac Systems) which measures breathing induced changes in pressure. The signal from this transducer went to a differential pressure signal conditioner (DA 100C, Biopac Systems), an A/D signal converter and was stored in digital form with Biopac System's MP100ACE data acquisition software. Biopac System's Acknowledge (v3.8.1) data acquisition program was used for data analysis. Outflow air then flowed into an open 150 ml syringe barrel. Air was sampled from this syringe barrel and drawn through an AEI Technologies CD-3A CO_2 analyzer and an AEI Technologies S-3A/I O_2 analyzer to measure O_2/CO_2 concentrations in the inspired air.

A mouse was placed individually into the chamber and was allowed to acclimate 30 minutes daily for 3 days prior to the testing. During the acclimation periods, room air flowed through the chamber continuously at ~500 ml/min. During both acclimation and testing periods, the chamber was placed in a water bath to help maintain a more constant temperature. On the testing day, a mouse was placed in the chamber and allowed to acclimate for 30 min with room air flowing through the chamber before testing began. At the end of the acclimation period, air flow was turned off for 1 min. This was followed by two periods of air flow for 5 min followed by no air flow for 1 min. The inflow air was then shifted from room air to 5% CO_2 containing air (derived from a tank containing gas with 5% CO_2, 21% O_2, and balance N_2) (hypercapnia). Exposure to hypercapnia consisted of 3 bouts of air flow on for 5 min followed by air flow off for 1 min. Following this 18 min session the mouse was exposed to hypercapnia for an additional 15 min with air flow on and then air flow was turned off for another 1 min period. The hypercapnia exposure was followed by a 15 min exposure to room air with air flow on followed by a 1 min period with air flow off. Lastly, two additional periods of room air exposure with air flow on for 5 min and off for 1 min each were conducted. Thus, the mouse was in the chamber for a total of 105 min. The air flow was checked during every airflow period and adjusted when necessary. The temperature of the chamber was measured three times during the experiment and the three values were averaged to derive a final value for the experiment. Three values for

water bath temperature were determined during the experiment using a glass thermometer and these values were averaged for “room” temperature. At the end of the experiment, inflow and outflow lines were turned off and several calibration injections of 100 µl air from a syringe were performed by first injecting air, then drawing the syringe back up and re-injecting, before finally removing the mouse from the chamber and measuring its body temperature rectally with a RET-3 Physitemp mouse rectal probe. The mouse was then weighed and returned to its housing. Ventilatory response of TDAG8 $^{+/+}$ and $^{-/-}$ mice to changes of inspired CO_2 levels from 0% (normocapnia) to 5% (hypercapnia) were measured.

Data Analysis: The pressure records were analyzed during the periods in which the airflow was off. We looked for segments of 3 or more seconds when ventilation was regular and no gross body movements were observed. The data were analyzed during awake states. For each mouse, while initially breathing room air we analyzed 2 to 3 segments of stable breathing with air flow off; while breathing 5% CO_2, we analyzed at least 1 stable breathing segment for each of the three 1 min air off periods which followed 5 min of hypercapnic air flow and for the last 1 min air off period following the 15 min period of hypercapnic air flow; upon return to breathing normocapnia we analyzed at least one stable breathing segment for each air off period. For each breathing segment, the respiratory parameters from the pressure signal (tidal volume (V_T), respiration frequency (F_R), and $V_E = V_T \times F_R$) were analyzed. In all cases, plethysmograph data were normalized to the weight of the mouse. F_R was calculated from the number of breathing pulses per time. V_T was calculated from the equation:

$$V_T = V_K \times P_T/P_K \times T_A/T_R \times (P_B - P_C)/[((P_B-P_C) - (T_A/T_b \times (P_B - P_R))]$$

Where V_K is the volume of the calibration injection (100 µl), P_T is the pressure deflection due to each breath, P_K is the pressure deflection associated with the injection of the calibration volume, T_A is the temperature in the animal chamber (average for all mice: 23.8 ± 0.4 °C), T_R is the temperature in the water bath (average for all mice: 22.7 ± 0.3 °C), P_B is the barometric pressure, P_C is the water vapor pressure at T_A, T_b is the body temperature of the mouse

(average for all mice: 36.2 ± 0.4 °C), and P_R is the water vapor pressure at T_b. The water vapor pressure at T_A and T_b were calculated using Antoine's Equation. The calculated value for V_T was multiplied by our calculated value for F_R for the same mouse to obtain minute ventilation. This was normalized for body mass by dividing by the mouse's body weight and multiplying by 100 g so that the final units for the V_e values were (mL/min)/100 g).

Immunofluorescence

Mice were perfused transcardially with 4.0% paraformaldehyde in 0.1M Na_2HPO_4 / NaH_2PO_4 buffer, pH 7.5. 30-µm coronal sections were sliced on microtome and stored at -20°C until processed for immunohistochemistry. Sections were removed from cryoprotectant and washed in 50 mM potassium PBS (KPBS, pH 7.2; 40 mM potassium phosphate dibasic, 10 mM potassium phosphate monobasic, and 0.9% sodium chloride) 5x for 5 min at room temperature. Next, the sections were treated with 1% H_2O_2 for 10 min and washed (5x 5 min in KPBS) to remove all H_2O_2, and incubated in blocking solution (0.1% bovine serum albumin, 0.2% Triton X-100 in KPBS) for 1 h. The sections were then placed in rabbit antibody to green fluorescent protein (GFP) (1:3000) in blocking solution overnight at 4°C. The next day the sections were washed (5x 5 min in KPBS) then incubated in biotinylated anti-rabbit IgG (1:500, Vector) in blocking solution for 1 h. Sections were then washed (5x 5 min in KPBS) and incubated in avidin-biotin complex (ABC, Vector Laboratories) at 1:1,000 in KPBS for 1 h. Sections were rinsed (5x 5 min in KPBS) and incubated for 10 min in biotin-labeled tyramide (PerkinElmer Life Sciences) diluted 1:250 in KPBS with 0.3% H_2O_2. Sections were again rinsed (5x 5 min in KPBS) and then incubated for 45 min in Cy3-conjugated Streptavidin (Jackson ImmunoResearch) diluted 1:200 in KPBS. Using GFP inserted downstream of the TDAG8 promoter (2), we characterized cellular localization of TDAG8 in brain tissue using triple label immunohistochemistry. For triple labeling, sections were washed (5x 5 min in KPBS) and incubated 1 h in blocking solution before incubation overnight at 4°C in the second primary

antibody (IBA-1 1:1000). Sections were washed (5x 5 min in KPBS) and incubated 45 min in Cy5-labeled anti-rabbit antibody diluted 1:200 in blocking solution. Sections were washed (5x 5 min in KPBS) and incubated 1 h in blocking solution before incubation overnight at 4°C in the third primary antibody (Huc/d (1:200) or GFAP (1:1000). Sections were washed (5x 5 min in KPBS) and incubated 45 min in Alexa-488-labeled anti-mouse (Huc/D) or anti-chicken (GFAP) antibody diluted 1:200 in blocking solution. Sections were then washed 3x in KPB and mounted out of a dish containing 0.3% aqueous gelatin onto Gold Seal UltraStick slides. Slides were dried at room temperature in complete darkness and then cover slipped using Gelvatol (Fluka).

Sections were imaged using an AxioImager Z1 microscope (Zeiss) equipped with apotome (z-stack) imaging capability (Axiocam MRm camera and AxioVision Release 4.6 software; Zeiss). All images were collected using a 20x or 40x air objective lens. Cy3 was excited using the 568 nm while 647 nm was used to collect images of Cy5-labeled cells. Co-localization was determined by overlapping signals. Brightness and contrast of the photomicrographs presented here were adjusted using Adobe Photoshop CS2 (San Jose, CA) to ensure the highest quality images for publication.

Morphological Analysis

Images from Iba1 positive cells at in the SFO (-0.22 mm to -0.82 mm from bregma) were acquired as Z-stacks. Flattened images were examined using Image J software (NIH open access) to quantify increased soma perimeter and attenuated microglial branching complexity and process length (de-ramification) that are parameters used for assessing microglial activation. The perimeter of the soma was measured using the ImageJ software tool “Freehand line”. Afterwards, this parameter was recorded using the ImageJ software option “Analyze and Measure”. Microglial branch length and number of endpoints were acquired using ImageJ software as described (3; 4). Briefly, images were enhanced so that all microglial branches were visible. Images were processed using ImageJ option “Despeckle” to remove single pixel

background staining and then converted into binary images and skeletonized. The “Analyze Skeleton” analysis was used to quantify the length and number of endpoints for each branch. These measures were then summed and normalized to the number of cells in each image.

Measurement of Cytokines

Mice were sacrificed via decapitation and snap frozen brains were stored at -80°C until dissection. SFO samples were micro-dissected from 2.3 mm slices on a cryostat (-20°C). Samples were homogenized in a dounce homogenizer with a tight fitting pestle in 500 ul of PBS supplemented with a cOmplete ULTRA protease inhibitor cocktail tablet (Roche). Samples were then centrifuged at 14,000 RPM for 15 min at 4°C and the supernatant was collected for cytokine analysis.

Preparation of Acute Brain Slices and Electrophysiology

Mice were anaesthetized, decapitated and the brains were quickly removed and chilled in ice-cold dissection buffer (250 mM glycerol, 2.5 mM KCl, 2.4 mM $CaCl_2$, 1.2 mM $MgCl_2$, 1.2 mM NaH_2PO_4, 26 mM $NaHCO_3$, 11 mM glucose, 0.5 mM ascorbic acid, equilibrated with 5% CO_2/95% O_2). The brain block was subsequently removed and placed onto a vibratome (Pelco Vibratome 1000). Coronal slices containing the SFO (300 μm) were cut in ice-cold dissection buffer and then incubated in a storage chamber containing artificial cerebrospinal fluid (aCSF) (3 mM KCl, 124 mM NaCl, 1.3 mM $MgSO_4$, 26 mM $NaHCO_3$, 1.25 mM NaH_2PO_4, 10 mM glucose, 2.4 mM $CaCl_2$, equilibrated with 5% CO_2/95% O_2) at room temperature for at least 30 min until being used.

In electrophysiological recordings, slices were placed on the floor of a perfusion chamber, held with a nylon grid, and continuously superfused with aCSF through stainless steel tubes via a gravity-fed system at a rate of 3-5 ml/min. SFO neurons were visualized with an

upright microscope (Nikon Optiphot-2) using near-infrared illumination and a 40x water-immersion objective (Hoffmann Modulated Contrast, N.A. 0.55, 3.0-mm working distance). All experiments were done at approximately 35°C, achieved by maintaining solution reservoirs in a 40ºC water bath and adjusted with an in-line thermoelectric Peltier assembly. Patch pipettes (3-6 MΩ) were pulled from thin-walled (1.5 mm outer diameter, 1.12 mm inner diameter) borosilicate glass capillaries (TW150-3, World Precision Instrument, Inc.) on a vertical electrode puller (Narishige PP-830). The internal pipette solution for the electrophysiological experiments contained 130 mM K-gluconate, 0.4 mM EGTA, 1 mM $MgCl_2$, 0.3 mM Na_2GTP, 2 mM Na_2ATP, 10 mM HEPES (pH 7.45). Membrane potential (V_m) and firing frequency were measured from whole-cell patched neuronal soma in current clamp mode. At least 15 min were required to equilibrate the intracellular solution with the internal pipette solution after the membrane was ruptured in the whole-cell configuration. A recording was used only if the neuron exhibited a resting membrane potential more negative than -45 mV and the amplitudes of action potentials were bigger than 60 mV. Occasionally, a small depolarizing DC current was injected into the cell to maintain an appropriate firing frequency. Electrical signals from individual neuronal soma were obtained in whole-cell patch clamp configuration with an Axopatch 200B amplifier, a Digidata 1440A A/D converter and pCLAMP 10.2 software (all from Molecular Devices Co.). An Ag-AgCl electrode connected to the bath solution via a KCl-agar bridge served as the reference electrode. Data were filtered at 2 kHz, sampled at 10 kHz, and analyzed offline. Membrane potentials were corrected for the liquid junction potential of 15 mV.

Protocol for repeated exposure control and IL-1RA experiments: To ensure reproducibility of CO_2 evoked responses we performed a repeated exposure control in SFO neurons (n = 4) from wild-type (WT) mice (Figure S10F). Baseline firing in normocapnia (5% CO_2) was recorded for ~5 minutes before exposing each neuron to hypercapnia (7.5% CO_2) for 5 minutes. Following the first CO_2 exposure, baseline firing recovered to near initial values in normocapnic aCSF. After a ~10-15 minute recovery period, the same neuron was exposed to

hypercapnia for a second time. In a separate series of experiments, SFO neurons (n = 5) from WT mice were subjected to the same protocol, except the second exposure to hypercapnia was performed in the presence of the IL-1β receptor antagonist, IL-1RA (experimental concentration; 200 ng/ml). IL-lRA was stored as 100 µg/ml stocks in PBS and 0.1% bovine serum albumin at −80°C. Stocks solutions were diluted to a final concentration of 200ng/ml for experiments.

Data Analysis: The spontaneous firing rates over a 1 min period before and during exposure to hypercapnic acid (7.5% CO_2 and 10% CO_2) were calculated to get the mean firing rate before, during and after exposure to hypercapnia. Changes in firing rate were analyzed using unpaired student's *t*-test.

Supplemental References

1. Ziemann AE, Allen JE, Dahdaleh NS, Drebot II, Coryell MW, Wunsch AM, *et al.* (2009): The amygdala is a chemosensor that detects carbon dioxide and acidosis to elicit fear behavior. *Cell*. 139: 1012–21.

2. Radu CG, Cheng D, Nijagal A, Riedinger M, McLaughlin J, Yang L V, *et al.* (2006): Normal immune development and glucocorticoid-induced thymocyte apoptosis in mice deficient for the T-cell death-associated gene 8 receptor. *Mol Cell Biol*. 26: 668–77.

3. Cutando L, Busquets-Garcia A, Puighermanal E, Gomis-González M, Delgado-García JM, Gruart A, *et al.* (2013): Microglial activation underlies cerebellar deficits produced by repeated cannabis exposure. *J Clin Invest*. 123: 2816–31.

4. Morrison HW, Filosa JA (2013): A quantitative spatiotemporal analysis of microglia morphology during ischemic stroke and reperfusion. *J Neuroinflammation*. 10: 4.